LETTERS

Boundary layer control of rotating convection systems

Eric M. King[1], Stephan Stellmach[2]†, Jerome Noir[1], Ulrich Hansen[2] & Jonathan M. Aurnou[1]

Turbulent rotating convection controls many observed features of stars and planets, such as magnetic fields, atmospheric jets and emitted heat flux patterns[1–6]. It has long been argued that the influence of rotation on turbulent convection dynamics is governed by the ratio of the relevant global-scale forces: the Coriolis force and the buoyancy force[7–12]. Here, however, we present results from laboratory and numerical experiments which exhibit transitions between rotationally dominated and non-rotating behaviour that are not determined by this global force balance. Instead, the transition is controlled by the relative thicknesses of the thermal (non-rotating) and Ekman (rotating) boundary layers. We formulate a predictive description of the transition between the two regimes on the basis of the competition between these two boundary layers. This transition scaling theory unifies the disparate results of an extensive array of previous experiments[8–15], and is broadly applicable to natural convection systems.

Rapidly rotating convection is typically organized by the Coriolis force into tall, thin, coherent convection columns that are aligned with the rotation axis (Fig. 1a). This organizing effect is thought, for example, to be responsible for the strength and structure of magnetic fields generated by convection in planetary interiors[16]. As thermal forcing is increased, the relative influence of rotation weakens, and three-dimensional, turbulent convection can occur (Fig. 1b). It is commonly assumed that rotational effects will dominate convection dynamics when the ratio of the global buoyancy force to the Coriolis forces is less than unity[7–12]. Here we argue, by means of a coupled set of laboratory and numerical experiments, that the boundary layer dynamics, not the global force balance, control the style of convection.

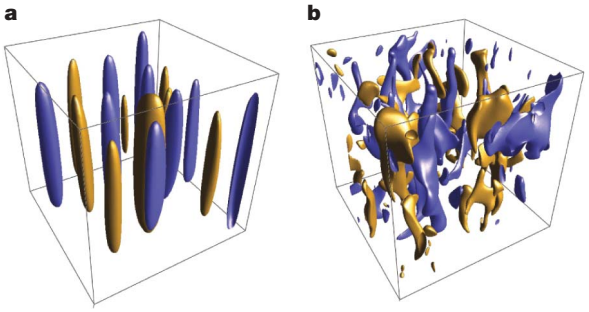

Figure 1 | Iso-surfaces of vertical velocity, from numerical experiments. **a**, $E = 10^{-4}$, $\mathrm{Ra} = 5 \times 10^6$, $\mathrm{Pr} = 7$. Here we see large-scale, coherent, axially aligned velocity structures typical of rotationally dominated convection. $\mathrm{Ro_c} = 0.08$, $\mathrm{Ra/Ra_t} = 0.36$. **b**, $E = 10^{-4}$, $\mathrm{Ra} = 2.1 \times 10^8$, $\mathrm{Pr} = 7$. Here we see predominantly three-dimensional convective structures typical of non-rotating convection, despite a ratio of global buoyancy to Coriolis force of $\mathrm{Ro_c} = 0.5$. However, the boundary-layer-transition hypothesis predicts this breakdown of rotational control, as $\mathrm{Ra/Ra_t} = 14$.

Many previous studies of heat transfer exist for rotating convection systems[8–10,12–15]. However, no unified description of rotating convective heat transfer exists. Often, such studies seek scaling laws for heat transfer efficiency as a function of thermal driving, $\mathrm{Nu} \propto \mathrm{Ra}^{\alpha}$. The Nusselt number, Nu, characterizes the efficiency of convective heat transfer, and is given by the ratio of the total heat transfer to the conductive heat transfer. Thus, $\mathrm{Nu} = 1$ for purely conductive heat transfer, and higher values of Nu correspond to more efficient convective heat transfer. The strength of buoyancy forcing is characterized by the ratio of buoyancy to diffusion, quantified by the Rayleigh number, Ra. In thermal convection, $\mathrm{Ra} = \alpha_T g \Delta T D^3/\nu\kappa$, where α_T is the fluid's thermal expansion coefficient, g is the acceleration due to gravity, ΔT is the temperature drop across the fluid layer, D is the length scale of the system, ν is the fluid's viscous diffusivity and κ is the fluid's thermal diffusivity. Many non-rotating convection studies yield a scaling exponent of $\alpha \approx 2/7$ (refs 10, 17, 18). Some rotating convection studies still find the $\alpha \approx 2/7$ scaling[8–10], whereas comparable studies have found a markedly different, $\alpha \approx 6/5$, scaling[12–14]. Extrapolating these two empirical scaling laws to astrophysical or geophysical parameters yields predictions that disagree by many orders of magnitude.

In this Letter, we show that this apparent discrepancy can be explained in terms of boundary layer dynamics. A convecting fluid volume consists of two distinct dynamical regions: the interior (or bulk) fluid, and the boundary layers[1,19]. Typically, most of the convecting volume is contained in the bulk, and the boundary layers are thin regions where the interior fluid meets the bounding surfaces and diffusion is important. In turbulent, non-rotating convection, diffusive effects are negligible in the bulk of the fluid. Ideally, strongly turbulent motions result in a well-mixed, isothermal interior, corresponding to an effective thermal short cut across the fluid layer[1]. The only remaining limitation to heat transfer, then, is in the quasi-static thermal boundary layers. In this system, it can be shown that $\mathrm{Nu} \propto D/\delta_\kappa$, where δ_κ is the thermal boundary layer thickness[1], such that the thermal boundary layer becomes thinner as the vigour of convection is increased (see Supplementary Information, section 2). In rotating fluid dynamics, the strength of rotation is characterized by the ratio of the viscous force to the Coriolis force, namely the Ekman number, $E = \nu/2\Omega D^2$, where Ω is the angular rate of rotation. In rapidly rotating systems, the important boundary layer is the Ekman layer, which promotes communication between the rotating container and the bulk fluid, permitting an interior flow that is controlled by rotation[9,19]. The Ekman boundary layer has thickness $\delta_E \propto E^{1/2}D$, such that the Ekman layer becomes thinner as the system's rotation rate increases.

Following refs 20–22, we hypothesize that the effects of rotation dominate convection dynamics when the Ekman layer is thinner than the thermal boundary layer, that is, when $\delta_E < \delta_\kappa$. By contrast, when

[1]Department of Earth and Space Sciences, University of California, Los Angeles, California 90095-1567, USA. [2]Institut für Geophysik, WWU Münster, AG Geodynamik Corrensstrasse 24, Münster 48149, Germany. †Present address: Department of Applied Mathematics and Statistics, and Institute of Geophysics and Planetary Physics, University of California, Santa Cruz, California 95064, USA.

the thermal boundary layer is thinner than the Ekman layer, $\delta_\kappa < \delta_E$, the uppermost part of the Ekman layer is mixed with the bulk. This mixing truncates the influence of the Ekman layer, and therefore rotation, on the interior fluid dynamics[20,22]. The transition between rotationally controlled and non-rotating convection dynamics therefore occurs when $\delta_\kappa \approx \delta_E$. We solve for a transitional Nusselt number scaling by equating δ_κ and δ_E, yielding $Nu_t \propto E^{-1/2}$. Thus, our hypothesis leads us to predict that convection will be dominated by the influence of rotation when $Nu < Nu_t$. Conversely, we expect non-rotating convection dynamics for $Nu > Nu_t$.

Rotating convection experiments allow us to vary the thickness of the thermal boundary layer by varying the heating rate, and that of the Ekman boundary layer by varying the rotation rate. To test our hypothesis, we carry out laboratory and numerical experiments spanning $2 \times 10^3 < Ra < 6 \times 10^9$ and $10^{-6} \leq E \leq \infty$ (see Supplementary Information, section 1). Heat transfer behaviour is shown in Fig. 2. Non-rotating ($E = \infty$) heat transfer data agree with the previously obtained $Nu \propto Ra^{2/7}$ scaling law[10,17,18]. Several different fluids are used, as characterized by the Prandtl number, $Pr = \nu/\kappa$. Fluids with different Prandtl numbers yield slightly different non-rotating scaling prefactors[23–25], but we do not consider this relatively weak effect here. When rotation is included, the onset of convection is delayed by the stabilizing effect of the Coriolis force[26]. Once convection begins, heat transfer exhibits a much steeper scaling, in agreement with the previously reported $Nu \propto Ra^{6/5}$ relationship[12–14]. More specifically, heat transfer is adequately described by $Nu = (Ra/Ra_c)^{6/5}$ in this convective regime, where $Ra_c = 6E^{-4/3}$ is the critical Rayleigh number for the onset of convection[26]. However, owing to the experimental limitations in accessing the rapidly rotating, strongly supercritical regime, this scaling is not well constrained. For strong enough thermal forcing (Ra) at a given rotation rate (E), our heat transfer data conform to the non-rotating scaling behaviour. Thus, we observe two distinct convective heat transfer regimes: the rotationally controlled regime, with $Nu \propto Ra^{6/5}$, and the non-rotating regime, with $Nu \propto Ra^{2/7}$.

We define the transition between these two regimes as the point of intersection between their respective scalings, $Nu = 0.16Ra^{2/7}$ and $Nu = (Ra/Ra_c)^{6/5}$. Equating the two, we solve for transitional Rayleigh and Nusselt numbers: $Ra_t = 1.4E^{-7/4}$ and $Nu_t = 0.18E^{-1/2}$. Figure 3a shows Nu normalized by the non-rotating scaling law versus Ra normalized by the transitional Rayleigh number. When $Ra < Ra_t$ ($Nu < Nu_t$), convection is constrained by the influence of rotation and heat transfer is less efficient than its non-rotating counterpart. When $Ra > Ra_t$ ($Nu > Nu_t$), heat transfer is not significantly affected by rotation and follows the non-rotating scaling. Indeed, our empirical results agree with the boundary layer transition hypothesis, which predicts that $Nu_t \propto E^{-1/2}$.

To further test our hypothesis, we measure the thicknesses of the two boundary layers from numerical experiments carried out at $E = 10^{-4}$ and $Pr = 7$ (Fig. 3b). Following refs 17, 27, we define the Ekman boundary layer thickness, δ_E, as the vertical position of the maximum value of the root-mean-square velocity, and the thermal boundary layer thickness, δ_κ, as the vertical position of the maximum value of the temperature variance (see Supplementary Information, section 2). Figure 3b illustrates that when $\delta_\kappa \approx \delta_E$, $Ra \approx Ra_t$ and the

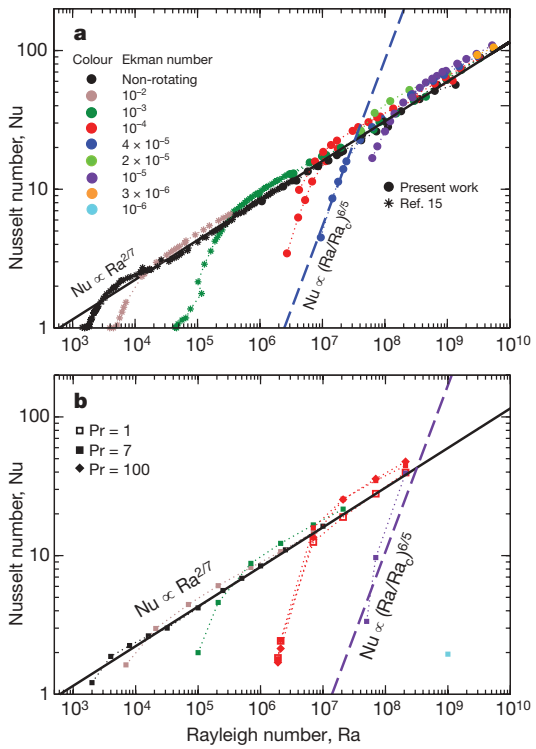

Figure 2 | Nusselt number versus Rayleigh number. **a**, Laboratory experiments; **b**, numerical simulations. Our laboratory experiments were carried out in cylinders with diameter-to-height ratios ranging from 6.25 to 1 using water ($Pr \approx 7$) and sucrose solution ($Pr \approx 10$). Included in **a** are results from ref. 15 in water. Numerical experiments are carried out in a Cartesian box with no-slip top and bottom boundaries and periodic sidewalls. Gravity and the rotation axis are both vertical. Non-rotating convection in laboratory experiments yields $Nu \propto Ra^{0.289 \pm 0.005}$ across more than five decades in Ra. Solid black lines represent the non-rotating scaling law $Nu = 0.16Ra^{2/7}$. Dashed black lines represent the rotationally controlled scaling law $Nu = (Ra/Ra_c)^{6/5}$, where $Ra_c = 6E^{-4/3}$ from ref. 26.

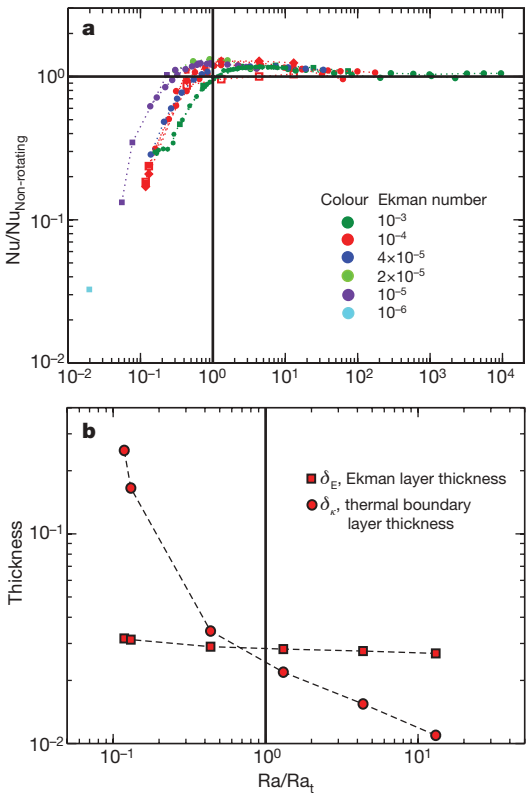

Figure 3 | The transition from rotationally controlled to non-rotating heat transfer behaviour. **a**, The heat transfer regime is determined by the transitional Rayleigh number, $Ra_t = 1.4E^{-7/4}$, for $E \leq 10^{-3}$ and $1 \leq Pr \leq 100$. Symbols are the same as in Fig. 2. The Nusselt number is normalized by its non-rotating value, $Nu_{Non\text{-}rotating} = 0.16Ra^{2/7}$. When $Ra/Ra_t > 1$, heat transfer follows the non-rotating scaling law. Near the transition, the data overshoot the non-rotating scaling law owing to Ekman pumping effects[9,30]. **b**, The numerically determined non-dimensional thicknesses of the competing boundary layers are shown as the Rayleigh number is varied for $E = 10^{-4}$ and $Pr = 7$. The dynamical transition at $Ra = Ra_t$ occurs when the relative thicknesses of the competing boundary layers are approximately equal, that is, when $\delta_\kappa = \delta_E$.

transition is in fact controlled by the relative thicknesses of the boundary layers. When the thermal boundary layer is thinner than the Ekman layer ($\delta_\kappa < \delta_E$, $Ra > Ra_t$), convection is manifested as turbulent, three-dimensional flow (Fig. 1b). Conversely, when the Ekman layer is thinner than the thermal boundary layer ($\delta_E < \delta_\kappa$, $Ra < Ra_t$), rotational effects control convection and constrain fluid motion (Fig. 1a).

It is often argued that the influence of rotation on turbulent convection dynamics is governed by the relative global magnitude of the relevant forces: the buoyancy force and the Coriolis force[7–12]. The ratio of these two global forces is represented by the convective Rossby number[7–12], $Ro_c = \sqrt{RaE^2\,Pr^{-1}}$. The force balance argument predicts a transition between rotationally controlled convection and non-rotating convection when $Ro_c \approx 1$ (see Supplementary Information, section 3), and thus predicts a transitional Rayleigh number that scales as E^{-2}, in comparison with the $E^{-7/4}$ scaling derived from our boundary layer arguments. These two scalings, when extrapolated to planetary settings, yield drastically different predictions for the importance of rotation. At a typical planetary value[12] of $E = 10^{-15}$, for example, the two scalings predict transitional Rayleigh numbers that differ by roughly four orders of magnitude. Figure 4 shows experimental heat transfer data (Nu) plotted against Ro_c. Should the force balance control the importance of rotation in convective heat transfer, we would expect the transitions to occur when $Ro_c \approx 1$. The heat transfer transitions observed in the data (Fig. 4) are not adequately explained by the global force balance, Ro_c, but are instead well described by our boundary-layer-controlled transition scaling. Furthermore, the force balance argument predicts a Pr-dependent transition, and no such dependence is observed. Our transition scaling also describes the disparate results from previous studies: those[12–14] finding the rotationally controlled $Nu \approx Ra^{6/5}$ heat transfer behaviour typically have $Ra < Ra_t$, whereas those[8–10] yielding the non-rotating scaling, $Nu \approx Ra^{2/7}$, typically have $Ra > Ra_t$, despite setting $Ro_c < 1$. To further test the validity of boundary layer control, future laboratory and numerical experiments must be able to access high Ra convection at lower values of E.

The boundary-layer-controlled transition scaling, Ra/Ra_t, is broadly applicable to natural convection systems (see Supplementary Information, section 4). The Rayleigh number, Ra, depends on a system's global density gradient (in thermal convection, the temperature gradient), which is often difficult to observe in nature. The flux-Rayleigh number, $Ra_f = RaNu$, depends instead on the overall buoyancy flux. For thermal convection, $Ra_f = \alpha_T g D^4 Q/\rho c_p \kappa^2 \nu$, where Q is the heat flux, ρ is the fluid's mean density and c_p is the fluid's specific heat. The product of Ra_t and Nu_t constitutes a transitional flux-Rayleigh number, $Ra_{f,t} = 0.25E^{-9/4}$.

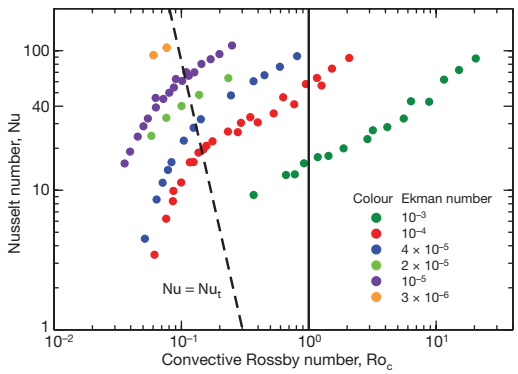

Figure 4 | Nusselt number versus the convective Rossby number for laboratory experiments in water ($Pr \approx 7$) with $3 \times 10^{-6} \leq E \leq 10^{-2}$. The convective Rossby number, Ro_c, characterizes the ratio of buoyancy forcing to the Coriolis force. Force balance arguments predict that rotation will dominate the system when $Ro_c < 1$. However, our heat transfer regime transitions follow the boundary-layer-controlled transitional Nusselt number, $Nu_t = 0.18E^{-1/2}$ (dashed line).

Thus, given the fluid properties, system size and rotation rate, as well as the emitted heat flux, a given body's convective regime can be determined. For example, a typical estimate[12,14] of the Ekman number in the Earth's liquid-metal outer core is $E \approx 10^{-15}$, which allows us to estimate a transitional flux-Rayleigh number of $Ra_{f,t} = 2 \times 10^{33}$ for the core. We estimate a flux-Rayleigh number of $Ra_f \approx 6 \times 10^{29}$ in the core using the following estimates[23,28]: $\alpha_T \approx 10^{-4}\,K^{-1}$; $g \approx 10\,m\,s^{-2}$; $D \approx 2 \times 10^6\,m$; $\rho \approx 10^4\,kg\,m^{-3}$; $c_p \approx 1{,}000\,J\,kg^{-1}\,K^{-1}$, $\kappa \approx 10^{-5}\,m^2\,s^{-1}$; $\nu \approx 10^{-6}\,m^2\,s^{-1}$; and a 4-TW superadiabatic heat flow from the core, corresponding to a superadiabatic $Q \approx 4 \times 10^{-2}\,W\,m^{-2}$. Using the empirical relation $Nu \approx (Ra/Ra_c)^{6/5}$, appropriate to convection with $Ra_f < Ra_{f,t}$, we provide the following estimate of the Rayleigh number in the Earth's core: $Ra \approx 7 \times 10^{24}$.

This estimate implies that core convection occurs just below the boundary layer transition, with $Ra/Ra_t \approx 3 \times 10^{-2}$, and this close proximity to the transition may be important for core dynamics. Recent work has shown that reversal frequencies of magnetic fields in dynamo simulations are linked to the decreasing importance of rotation[29]. Geomagnetic reversals may then depend on boundary layer dynamics and on the value of Ra/Ra_t in the core. To test the planetary and stellar applicability of our result, future work must investigate the influence of low-Pr fluids, fluid compressibility, strong magnetic fields, spherical geometry and internal heating on the boundary layer transition.

Received 27 June; accepted 28 October 2008.

1. Spiegel, E. A. Convection in stars. *Annu. Rev. Astron. Astrophys.* **9,** 323–353 (1971).
2. Ingersoll, A. P. & Porco, C. C. Solar heating and internal heat flow on Jupiter. *Icarus* **35,** 27–43 (1978).
3. Hathaway, D. H. A convective model for turbulent mixing in rotating convection zones. *Astrophys. J.* **276,** 316–324 (1984).
4. Busse, F. H. Convective flows in rapidly rotating sphere and their dynamo action. *Phys. Fluids* **14,** 1301–1314 (2002).
5. Heimpel, M., Aurnou, J. & Wicht, J. Simulation of equatorial and high-latitude jets on Jupiter in a deep convection model. *Nature* **438,** 193–196 (2005).
6. Aurnou, J., Heimpel, M., Allen, L., King, E. & Wicht, J. Convective heat transfer and the pattern of thermal emission on the gas giants. *Geophys. J. Int.* **173,** 793–801 (2008).
7. Gilman, P. A. Nonlinear dynamics of Boussinesq convection in a deep rotating spherical shell. *Geophys. Astrophys. Fluid Dyn.* **8,** 93–135 (1977).
8. Julien, K., Legg, S., McWilliams, J. & Werne, J. Hard turbulence in rotating Rayleigh-Bénard convection. *Phys. Rev. E* **53,** 5557–5560 (1996).
9. Julien, K., Legg, S., McWilliams, J. & Werne, J. Rapidly rotating turbulent Rayleigh-Bénard convection. *J. Fluid Mech.* **322,** 243–273 (1996).
10. Liu, Y. & Ecke, R. E. Heat transport in turbulent Rayleigh-Bénard convection: effects of rotation and Prandtl number. *Phys. Rev. Lett.* **79,** 2257–2260 (1997).
11. Aurnou, J. M., Heimpel, M. & Wicht, J. The effects of vigorous mixing in a convective model of zonal flow on the ice giants. *Icarus* **190,** 110–126 (2007).
12. Aurnou, J. M. Planetary core dynamics and convective heat transfer scaling. *Geophys. Astrophys. Fluid Dyn.* **101,** 327–345 (2007).
13. Christensen, U. R. Zonal flow driven by strongly supercritical convection in rotating spherical shells. *J. Fluid Mech.* **470,** 115–133 (2002).
14. Christensen, U. R. & Aubert, J. Scaling properties of convection-driven dynamos in rotating spherical shells and application to planetary magnetic fields. *Geophys. J. Int.* **166,** 97–114 (2006).
15. Rossby, H. T. A study of Bénard convection with and without rotation. *J. Fluid Mech.* **36,** 309–335 (1969).
16. Olson, P. L. & Christensen, U. R. Dipole moment scaling for convection-driven planetary dynamos. *Earth Planet. Sci. Lett.* **250,** 561–571 (2006).
17. Takeshita, T., Segawa, T., Glazier, J. A. & Sano, M. Thermal turbulence in mercury. *Phys. Rev. Lett.* **76,** 1465–1468 (1996).
18. Glazier, J. A., Segawa, T., Naert, A. & Sano, M. Evidence against ultrahard thermal turbulence at very high Rayleigh numbers. *Nature* **398,** 307–310 (1999).
19. Greenspan, H. P. *The Theory of Rotating Fluids* (Cambridge Univ. Press, 1968).
20. Hignett, P., Ibbetson, A. & Killworth, P. D. On thermal rotating convection driven by non-uniform heating from below. *J. Fluid Mech.* **109,** 161–187 (1981).
21. Boubnov, B. M. & Golitsyn, G. S. Temperature and velocity field regimes of convective motions in a rotating plane fluid layer. *J. Fluid Mech.* **219,** 215–239 (1990).
22. Read, P. L. Transition to geostrophic turbulence in the laboratory, and as a paradigm in atmospheres and oceans. *Surv. Geophys.* **22,** 265–317 (2001).
23. Tilgner, A. High-Rayleigh-number convection in spherical shells. *Phys. Rev. E* **53,** 4847–4851 (1996).
24. Verzicco, R. & Camussi, R. Prandtl number effects in convective turbulence. *J. Fluid Mech.* **383,** 55–73 (1999).

25. Schmalzl, J., Breuer, M. & Hansen, U. The influence of the Prandtl number on the style of vigorous thermal convection. *Geophys. Astrophys. Fluid Dyn.* **96,** 381–403 (2002).
26. Chandrasekhar, S. The instability of a layer of fluid heated below and subject to Coriolis forces. *Proc. R. Soc. Lond. A* **217,** 306–327 (1953).
27. Belmonte, A., Tilgner, A. & Libchaber, A. Temperature and velocity boundary layers in turbulent convection. *Phys. Rev. E* **50,** 269–279 (1994).
28. Nimmo, F., Price, G. D., Brodholt, J. & Gubbins, D. The influence of potassium on core and geodynamo evolution. *Geophys. J. Int.* **156,** 363–376 (2004).
29. Kutzner, C. & Christensen, U. R. From stable dipolar towards reversing numerical dynamos. *Phys. Earth Planet. Inter.* **131,** 29–45 (2002).
30. Kunnen, R. P. J., Clercx, H. J. H. & Geurts, B. J. Heat flux intensification by vortical flow localization in rotating convection. *Phys. Rev. E* **74,** 056306 (2006).

Supplementary Information is linked to the online version of the paper at www.nature.com/nature.

Acknowledgements Salary support for E.M.K., J.N. and J.M.A. was provided by the US National Science Foundation Earth Sciences Division Geophysics Program and the NASA Planetary Atmospheres Program. Support for S.S. and U.H. was provided by the German Research Foundation and for S.S. by the NASA Solar and Heliospheric Physics Program. Support for laboratory experiment fabrication was provided by the US National Science Foundation Instrumentation & Facilities Program. Computational resources were provided by the John von Neumann-Institut für Computing. E.M.K., J.N. and J.M.A. would like to thank J. Frydman, J. Neal, A. Yaghmaei and R. M. Aurnou for engineering support in experimental development. E.M.K. and J.M.A. would like to thank H. T. Rossby for making his thesis data available to them, J. McWilliams for discussion and S. R. Dickman for introducing them to geophysics.

Author Information Reprints and permissions information is available at www.nature.com/reprints. Correspondence and requests for materials should be addressed to E.M.K. (eric.king@ucla.edu).